# A Novel Major Facilitator Superfamily Protein at the Tonoplast Influences Zinc Tolerance and Accumulation in Arabidopsis[1][C][W][OA]

**Michael J. Haydon and Christopher S. Cobbett***

Department of Genetics, University of Melbourne, Parkville, Victoria 3010, Australia

Zinc (Zn) is an essential micronutrient required by all cells but is toxic in excess. We have identified three allelic Zn-sensitive mutants of Arabidopsis (*Arabidopsis thaliana*). The gene, designated *ZINC-INDUCED FACILITATOR1* (*ZIF1*), encodes a member of the major facilitator superfamily of membrane proteins, which are found in all organisms and transport a wide range of small, organic molecules. Shoots of *zif1* mutants showed increased accumulation of Zn but not other metal ions. In combination with mutations affecting shoot-to-root Zn translocation, *zif1 hma2 hma4* triple mutants accumulated less Zn than the wild type but remained Zn sensitive, suggesting that the *zif1* Zn-sensitive phenotype is due to altered Zn distribution. *zif1* mutants were also more sensitive to cadmium but less sensitive to nickel. *ZIF1* promoter-$\beta$-glucuronidase fusions were expressed throughout the plant, with strongest expression in young tissues, and predominantly in the vasculature in older tissues. *ZIF1* expression was highly induced by Zn and, to a lesser extent, by manganese. A ZIF1-green fluorescent protein fusion protein localized to the tonoplast in transgenic plants. MTP1 has been identified as a tonoplast Zn transporter and a *zif1-1 mtp1-1* double mutant was more sensitive to Zn than either of the single mutants, suggesting ZIF1 influences a distinct mechanism of Zn homeostasis. Overexpression of *ZIF1* conferred increased Zn tolerance and interveinal leaf chlorosis in some transgenic lines in which *ZIF1* expression was high. We propose that ZIF1 is involved in a novel mechanism of Zn sequestration, possibly by transport of a Zn ligand or a Zn ligand complex into vacuoles.

Zinc (Zn) is an essential micronutrient that, in eukaryotes, fulfills a structural role in over 300 enzymes (Vallee and Auld, 1990) and in many Zn-finger proteins involved in signaling and transcriptional regulation (Berg and Shi, 1996). In excess, Zn is also toxic to cells, presumably due to competition with other biologically important ions, which in plants ultimately leads to reduced biomass, leaf chlorosis, and root inhibition. Plants have mechanisms for Zn homeostasis and are able to respond to excess Zn through Zn tolerance mechanisms, including exclusion from the root or, within the plant, transport into specific tissues, cellular or subcellular compartments, or sequestration by Zn-binding ligands (Clemens, 2001). The role of membrane transporters is central to Zn homeostasis, being required for uptake, compartmentalization, vascular loading, and delivery into organelles for utilization, and a number of protein families have been implicated in Zn transport in plants.

The first Zn transporters identified in plants were the Zrt-, Irt-like proteins (ZIPs) from Arabidopsis by functional complementation of a Zn uptake-deficient yeast (*Saccharomyces cerevisiae*) strain (Grotz et al., 1998). *ZIP1* and *ZIP3* were shown to be induced in roots of Zn-starved seedlings, and *ZIP4* was highly expressed in shoots and roots of Zn-deficient plants. Microarray analysis of Arabidopsis has demonstrated that a number of genes encoding ZIP proteins are induced in plants grown under Zn-deficient conditions (Wintz et al., 2003). Plant ZIP proteins that mediate uptake of Zn into yeast have also been identified in rice (*Oryza sativa*), soybean (*Glycine max*), *Medicago truncatula*, and the Zn-cadmium (Cd) hyperaccumulator *Thlaspi caerulescens* (Pence et al., 2000; Moreau et al., 2002; Lopez-Millan et al., 2004; Ishimaru et al., 2005). There are 18 genes predicted to encode ZIPs in Arabidopsis (Gaither and Eide, 2001) and, although the physiological functions of Zn-transporting ZIPs are yet to be described in plants, they are predicted to be involved in cellular uptake, including across the root plasma membrane, and in mobilization of stored Zn.

The P-type ATPases are a superfamily of ATP-driven ion transporters that have been divided into subfamilies based on sequence similarity and substrate specificity (Axelsen and Palmgren, 2001). The type $1_B$ subfamily of P-type ATPases transport heavy metal ions and sequence comparisons can divide these into two distinct classes that reflect the substrate specificity for

[1] This work was supported by the Australian Research Council and the Albert Shimmins Fund (financial support to M.J.H. during preparation of the manuscript).

* Corresponding author, e-mail ccobbett@unimelb.edu.au; fax 61–3–8344–5138.

The author responsible for distribution of materials integral to the findings presented in this article in accordance with the policy described in the Instructions for Authors (www.plantphysiol.org) is: Chris Cobbett (ccobbett@unimelb.edu.au).

[C] Some figures in this article are displayed in color online but in black and white in the print edition.

[W] The online version of this article contains Web-only data.

[OA] Open Access articles can be viewed online without a subscription.

www.plantphysiol.org/cgi/doi/10.1104/pp.106.092015

monovalent cations, such as $Cu^+$ or $Ag^+$, or divalent cations, such as $Zn^{2+}$, $Cd^{2+}$, $Pb^{2+}$, or $Co^{2+}$ (Cobbett et al., 2003). There are eight type $1_B$ P-type ATPases in *Arabidopsis thaliana* and three, HMA2, HMA3, and HMA4, transport $Zn^{2+}$ or $Cd^{2+}$ when expressed in *Escherichia coli* or yeast (Mills et al., 2003; Eren and Arguello, 2004; Gravot et al., 2004; Verret et al., 2005). *HMA2* and *HMA4* are expressed in vascular tissues of roots, leaves, and flowers and protein-green fluorescent protein (GFP) fusions localize to the plasma membrane (Hussain et al., 2004; Verret et al., 2004). Analysis of T-DNA mutants demonstrated that, although neither single mutant presented an obvious phenotype, *hma2 hma4* double mutants exhibited leaf chlorosis, were stunted and infertile, and accumulated low levels of Zn in shoots despite elevated Zn content in roots (Hussain et al., 2004). The phenotype could be rescued by supplementation with Zn, suggesting that these mutants were Zn deficient due to impaired root-to-shoot translocation of Zn. Overexpression of HMA4 in Arabidopsis can increase transport of Zn to aerial tissues (Verret et al., 2004), and it has been proposed that HMA2 and HMA4 function, at least partially redundantly, in loading and/or unloading of Zn in vascular tissues for long-distance transport. The function of HMA3 in planta is not yet understood. Expression in yeast conferred Cd tolerance, despite similar Cd concentration to controls, implying a role in subcellular sequestration consistent with HMA3-GFP localization to vacuoles in yeast (Gravot et al., 2004). Localization of HMA3 in *A. thaliana* is not known but expression is normally low (Becher et al., 2004), and, in the Columbia (Col) ecotype, *HMA3* contains a frameshift mutation that would lead to a truncated protein and is presumed to be nonfunctional (Cobbett et al., 2003). Orthologs of the Zn-transporting P-type ATPases have been identified in the Zn-Cd hyperaccumulators *T. caerulescens* and *Arabidopsis halleri*. *TcHMA4* was identified from a cDNA library screen in yeast for Cd tolerance and can transport Zn, Cd, and lead (Pb) out of yeast cells (Papoyan and Kochian, 2004). *AhHMA3* and *AhHMA4* have been identified as transcripts expressed at elevated levels in *A. halleri* compared to *A. thaliana*, and both confer Zn tolerance when expressed in yeast (Becher et al., 2004, Talke et al., 2006). In addition, there are eight type $1_B$ P-type ATPases in the rice genome (Baxter et al., 2003). Based on protein sequence comparisons, only two, OsHMA2 and OsHMA3, are predicted to transport Zn.

Cation diffusion facilitators (CDFs) have been described in Arabidopsis that contribute to Zn tolerance by vacuolar Zn sequestration. *MTP1* (formerly *ZAT1*) is expressed constitutively in both roots and shoots and confers a moderate increase in Zn tolerance when overexpressed (van der Zaal et al., 1999). MTP1 transports Zn in proteoliposomes and Xenopus oocytes (Bloss et al., 2002; Desbrosses-Fonrouge et al., 2005), and GFP fusions and western blots using membrane fractions show MTP1 is in the tonoplast in *A. thaliana* (Kobae et al., 2004; Desbrosses-Fonrouge et al., 2005). Mutation or RNAi-mediated knockdown of *AtMTP1* confers increased sensitivity to excess Zn, indicating that MTP1 is likely to play a key role in Zn tolerance (Kobae et al., 2004; Desbrosses-Fonrouge et al., 2005). More recently, *AtMTP3* has been identified as a second tonoplast-localized CDF that also confers moderate Zn tolerance when overexpressed and increased Zn sensitivity in RNAi lines (Arrivault et al., 2006). Unlike *MTP1*, *MTP3* is predominantly expressed in roots and is induced by high Zn, manganese (Mn), and cobalt (Co), as well as iron (Fe) deficiency. It was suggested that MTP3 is important for sequestration of Zn in root vacuoles under elevated Zn, as well as Fe deficiency (Arrivault et al., 2006). In leaves of both *A. halleri* and *T. caerulescens*, genes encoding CDF transporters are more highly expressed than in nonaccumulator species (Becher et al., 2004; Hammond et al., 2006). AhMTP1 localized to the tonoplast in *A. thaliana* protoplasts and Zn tolerance and elevated *MTP1* transcript cosegregated with duplicated copies of *MTP1* in backcrossed populations, indicating an important role for MTP1 in Zn tolerance in the hyperaccumulator *A. halleri* (Drager et al., 2004).

An additional transporter has been identified in plants that can transport Zn. AtMHX was cloned from Arabidopsis by PCR based on sequence similarity to a mammalian $Na^+$-$Ca^{2+}$ exchanger, but was shown to transport $Mg^{2+}$ and $Zn^{2+}$ by proton antiport and localized to vacuoles (Shaul et al., 1999). The importance of this transporter for Zn homeostasis in *A. thaliana* is not clear, although expression of MHX in *A. halleri* is elevated compared to *A. thaliana* and may be important for Zn tolerance in this species (Elbaz et al., 2006).

In this study, a Zn-sensitive mutant, *zinc-induced facilitator1* (*zif1*), has been identified. *ZIF1* encodes a major facilitator superfamily (MFS) transporter with low similarity to any previously characterized protein. ZIF1, like MTP1, MTP3, and MHX, is localized to the tonoplast and identifies a novel component of Zn homeostasis in plants.

## RESULTS

### Mutations Affecting a MFS Protein Confer Zn Sensitivity

A Zn-sensitive T-DNA insertion mutant, designated *zif1-1*, was identified in the Wassilewskija (Ws) ecotype of *A. thaliana* in the process of identifying mutants for a previous study (Hussain et al., 2004). Inverse PCR revealed the T-DNA to be in a gene (At5g13740) encoding an MFS protein. The mutant was backcrossed to Ws and, from an F2 population that segregated for kanamycin resistance in a 3:1 ratio, 24 unselected F3 populations were genotyped for the T-DNA insertion by PCR and scored for kanamycin resistance and the Zn-sensitive phenotype. Cosegregation of the T-DNA, kanamycin resistance, and Zn sensitivity were observed in all populations and were consistent with a

single T-DNA insertion site. A second T-DNA allele, *zif1-2*, was obtained in the Col ecotype from the SALK collection (SALK_011408) and an individual homozygous for the T-DNA insertion was backcrossed to Col. In the F2 progeny, Zn sensitivity segregated in a Mendelian ratio, although kanamycin resistance was too weak to score. In addition, we conducted a screen of ethyl methanesulfonate-mutagenized Col M2 seed to identify additional mutants with a Zn-sensitive phenotype similar to that of *zif1-1*. One mutant, *zif1-3*, failed to complement *zif1-2* in both F1 and F2 individuals, and nucleotide sequencing of the entire coding region of *ZIF1* in *zif1-3* individuals revealed a single base pair change resulting in a G472R substitution in the predicted 12th transmembrane domain (TMD). Backcrossed, homozygous populations of the three mutants were used for all experiments.

The locations of the mutations in *zif1* mutants are summarized in Figure 1A. Because the T-DNA is inserted into an intron in both *zif1-1* and *zif1-2*, it was important to test whether these are true knockout mutants. Reverse transcription (RT)-PCR using primers that flank the T-DNA insertion sites showed that no wild-type transcript could be detected in *zif1-1*, whereas a decreased level of truncated transcript (approximately 25%) was detected by amplifying a region upstream of the insertion site (Fig. 1B). In contrast, low levels of wild-type transcript could be amplified from *zif1-2* seedlings (Fig. 1B) using either primers flanking the insertion site or primers specific for a downstream region. The identity of the product was confirmed by digestion at a predicted restriction site (data not shown). Using the primers for the downstream region, the level of wild-type transcript in *zif1-2* was estimated as approximately 6% of that in Col (Fig. 1B).

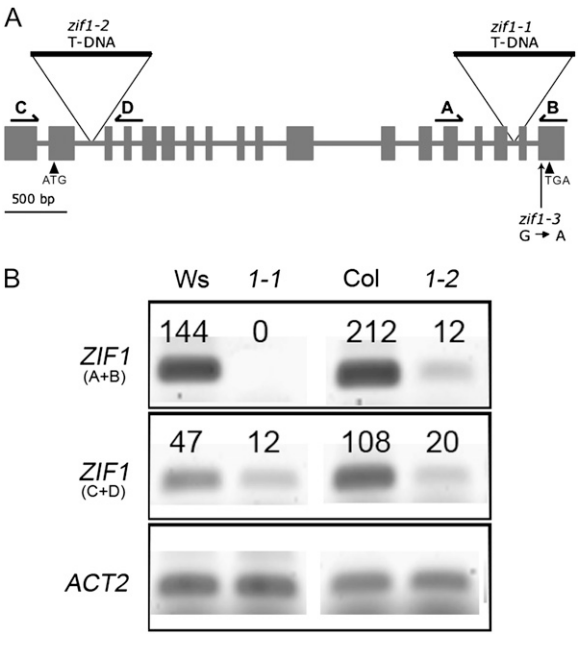


**Figure 1.** Molecular analysis of T-DNA knockouts. A, Schematic representation of *ZIF1* showing approximate locations of exons (gray boxes), introns (black lines), and translational initiation and termination codons (arrowheads) constructed from information available from The Arabidopsis Information Resource (TAIR; www.arabidopsis.org). The experimentally determined locations of the T-DNA insertions in *zif1-1* and *zif1-2* and the single base pair substitution in *zif1-3* are indicated. Two primer pairs were designed to flank the T-DNA in *zif1-1* (A + B) and *zif1-2* (C + D). B, RT-PCR of Ws, *zif1-1* (*1-1*), Col, and *zif1-2* (*1-2*) using A + B primers (24 cycles), C + D primers (26 cycles), or *ACT2* primers (18 cycles). Gels were stained with SYBR Green I. Numbers represent percent abundance relative to *ACT2* determined using ImageQuant software.

The three *zif1* mutants showed similar levels of sensitivity to Zn compared to the wild type (Fig. 2A). The sensitivity is characterized by increased chlorosis and decreased shoot fresh weight and root length compared to the corresponding wild-type controls. When grown on medium containing 60 $\mu$M Zn, *zif1-1*, *zif1-2*, and *zif1-3* had 51%, 55%, and 39%, respectively, of the shoot fresh weight of the wild type (Fig. 2B). Similarly, on 100 $\mu$M Zn, the root length of *zif1* mutants was 30% to 36% of that on control medium, whereas the wild types were unaffected (Fig. 2C).

The sensitivity of *zif1* mutants to other metals was also tested. The three mutants showed increased sensitivity to Cd, with increased chlorosis (Fig. 3A) and decreased shoot and root fresh weight (Fig. 3, B and C), although root length was not inhibited at the concentrations of Cd used (data not shown). On medium containing inhibitory levels of nickel (Ni), mutant plants appeared to have decreased sensitivity (Fig. 3D), evident in increased shoot fresh weight (Fig. 3E) and decreased root inhibition (Fig. 3F). No significant differences in shoot fresh weight, root length, or leaf chlorosis were observed between *zif1* mutants and wild-type plants when grown on a range of inhibitory concentrations of Cu, Co, Mn, or Fe (data not shown).

MFS proteins have been identified in all organisms from bacteria to mammals. They contain either 12 or 14 TMDs, with a large, cytoplasmic loop between TMD6 and TMD7, and a conserved MFS-specific motif between TMD2 and TMD3. Substrates are typically small, organic molecules, such as sugars, amino acids, and organic acids, and transport occurs via symport, antiport, or uniport (Pao et al., 1998). Of the MFS members that have been characterized, ZIF1 is most similar to the drug-$H^+$ antiporters from bacteria, although the amino acid sequence similarity is less than 40%. There are more than 90 genes in *A. thaliana* that code for putative MFS proteins (Ren and Paulsen, 2005), and the limited number of these that have been characterized transport sugars (Sauer and Stolz, 1994; Stolz et al., 1994), phosphate (Muchhal et al., 1996; Smith et al., 1997), or nitrate (Tsay et al., 1993). There are putative ZIF1 orthologs, based on high amino acid sequence similarity, in other plant species. Two, which share 67% sequence similarity with ZIF1, have been identified in maize (*Zea mays*; Simmons et al., 2003). There are at least five orthologs in the rice genome that are between 60% and 70% similar, and one

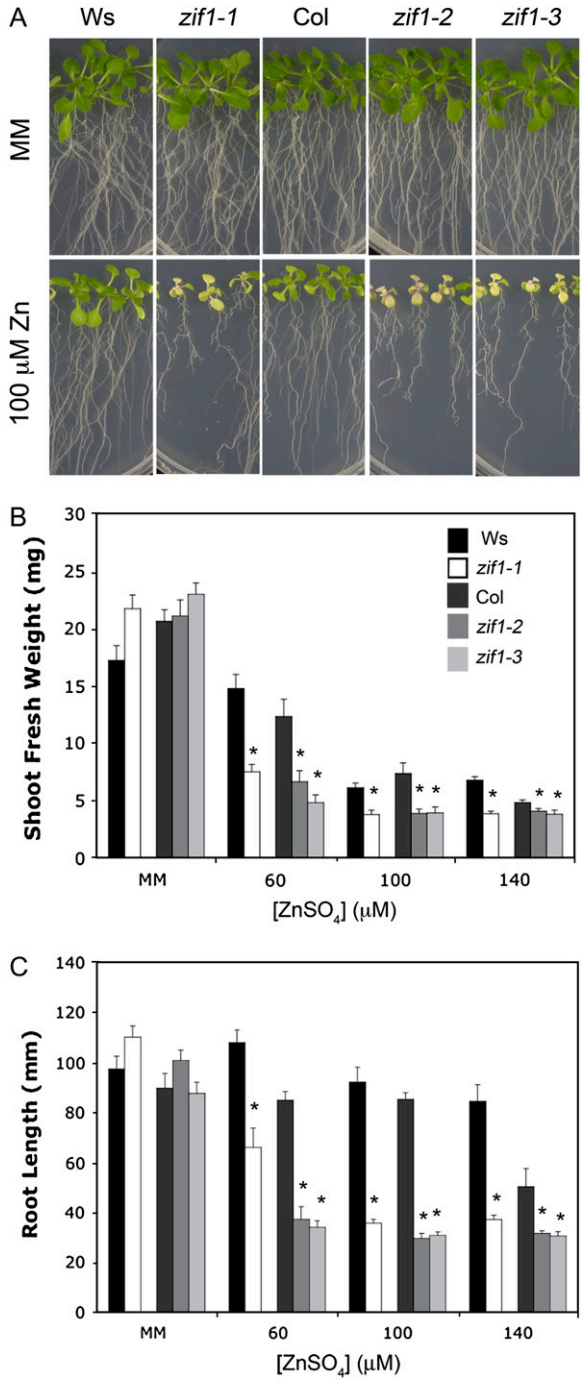


**Figure 2.** Zn sensitivity of *zif1* alleles. A, Seventeen-day-old Col, *zif1-1*, *zif1-2*, and *zif1-3* plants growing vertically on MM or MM containing 100 $\mu$M $ZnSO_4$. B, Shoot fresh weight. C, Root length. Seven-day-old plants were transferred from MM to MM containing the indicated metal concentration and grown vertically for a further 10 d as described in "Materials and Methods." Values are mean ± SE ($n = 8$). Statistical differences from Col were determined by *t* test (*, $P < 0.05$). [See online article for color version of this figure.]

orthologous sequence, which shares 73% protein sequence similarity with ZIF1, has been identified in red clover (*Trifolium pratense*). Although the function of these is unknown, they, along with ZIF1, are predicted to contain 12 TMD and possess the MFS signature sequence and conserved motifs believed to be important for proton-substrate antiport (Simmons et al., 2003).

In the Arabidopsis genome, there are two *ZIF1* paralogs that we have designated *ZIF-LIKE1* (*ZIFL1*; At5g13750) and *ZIFL2* (At3g43790). ZIFL1 and ZIFL2 share 80% and 75% amino acid sequence similarity with ZIF1, respectively. To investigate the role of these genes in Zn tolerance, T-DNA mutants were obtained from the SALK collection: SALK_030680 (*zifl1-1*) and SALK_059042 (*zifl2-1*). Homozygous individuals were identified by PCR and backcrossed to the wild type. F2 populations were scored for kanamycin resistance and homozygous mutant individuals were identified from populations that showed 3:1 segregation of the marker. Using RT-PCR, no wild-type transcript could be detected from each gene in the corresponding mutant (data not shown). To address the possibility of functional redundancy, *zif1-2 zifl2-1* and *zif1-1 zifl2-1* double mutants were generated. *ZIF1* and *ZIFL1* are tandem genes so the double mutant could not be generated. The single and double mutants were tested for sensitivity to Zn. With respect to leaf chlorosis and fresh weight, the single mutants, *zifl1-1* and *zifl2-1*, and the *zifl1-1 zifl2-1* double mutant were not different from the wild type, and the *zif1-2 zifl2-1* mutant was not different from *zif1-2* (data not shown). This suggests that, at least at the whole-plant level, these mutations do not contribute to a Zn sensitivity phenotype.

### *zif1* Mutants Accumulate Elevated Levels of Zn

To investigate whether the Zn-sensitive phenotype of *zif1* mutants is associated with increased accumulation of Zn, the shoot metal content of Ws wild-type and *zif1-1* plants was determined using inductively coupled plasma-atomic emission spectrometry (ICP-AES). When plants were grown on mineral salts medium (MM) from which Zn had been omitted, there was no difference in shoot Zn content in *zif1-1* compared to the wild type (Fig. 4A). However, when grown on MM containing 10 $\mu$M $ZnSO_4$, *zif1-1* shoots contained 32% more Zn than Ws (Fig. 4B). A significant increase in shoot Fe content was also observed in *zif1-1* plants compared to Ws when grown on MM without Zn, but there was no difference between shoot Fe content of Ws and *zif1-1* plants when grown on MM with 10 $\mu$M Zn (Fig. 4, A and B). No significant differences in shoot content of Mn, copper (Cu; Fig. 4, A and B), magnesium (Mg), or calcium (Ca; data not shown) between *zif1-1* and Ws plants grown on either medium were detected.

To confirm these observations, the metal content in shoots and roots of Col wild-type and *zif1-2* seedlings grown on MM, which contains 1 $\mu$M Zn, or MM with

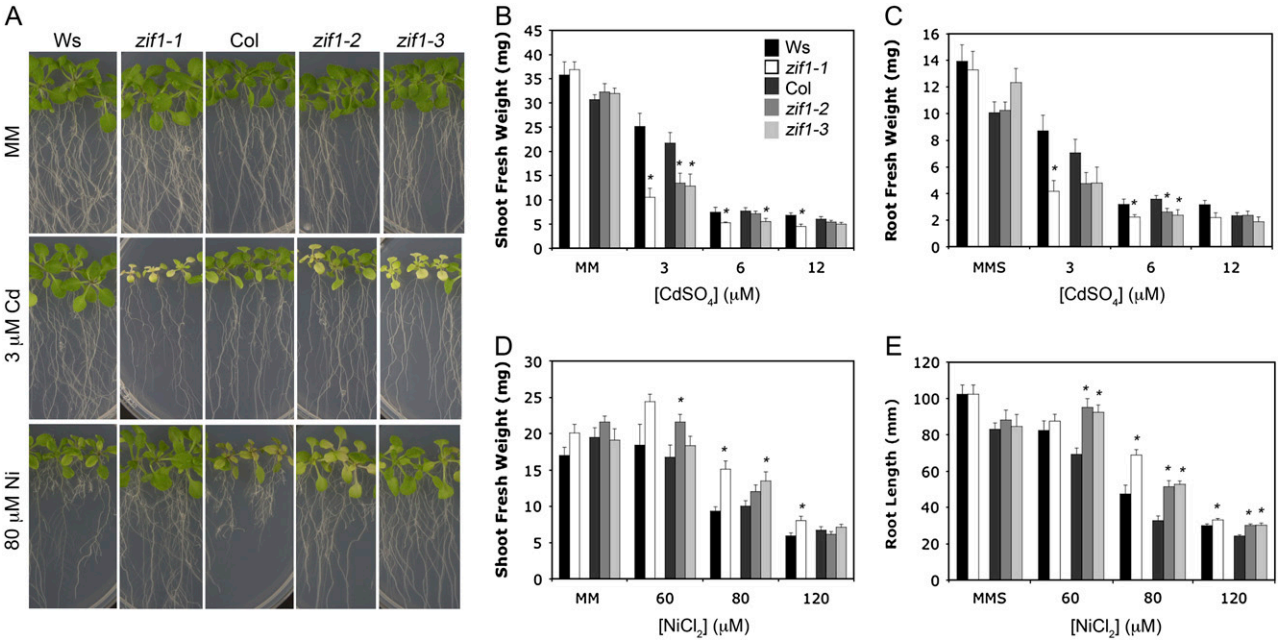


**Figure 3.** Cd sensitivity and Ni tolerance of *zif1* alleles. A, Seventeen-day-old Col, *zif1-1*, *zif1-2*, and *zif1-3* plants growing vertically on MM or MM containing 3 $\mu$M $CdSO_4$ or 80 $\mu$M $NiCl_2$. B and D, Shoot fresh weight. C and E, Root length. Seven-day-old plants were transferred from MM to MM containing the indicated metal concentration and grown vertically for a further 10 d. Values are mean ± SE ($n = 8$). Statistical differences from Col were determined by *t* test (*, $P < 0.05$). [See online article for color version of this figure.]

30 or 60 $\mu$M Zn added was determined. There was no significant difference between shoot Zn content of Col and *zif1-2* plants when grown on MM (Fig. 4C), but moderate increases in shoot Zn content of 13% and 41% were detected in *zif1-2* seedlings grown on medium containing 30 or 60 $\mu$M Zn, respectively, compared to the wild type. In a separate experiment, shoot Zn content was also significantly increased in *zif1-1* seedlings compared to Ws wild type when grown on medium containing 30 or 60 $\mu$M Zn by 23% and 47%, respectively, but was not significantly different when grown on MM (Fig. 4D). Similarly, root Zn content of *zif1-2* was not different from Col when grown on MM, but was significantly higher in *zif1-2* plants grown on 30 or 60 $\mu$M Zn by 36% and 88%, respectively (data not shown). No significant differences in Mn content of Col and *zif1-2* were observed in roots or shoots of seedlings grown on MM or medium containing 30 $\mu$M Zn. However, in plants grown on medium containing 60 $\mu$M Zn, Mn content was 89% and 48% higher in *zif1-2* shoots and roots, respectively, compared to wild type (data not shown). No significant differences in Fe, Cu, Mg, Ca, or potassium (K) content in roots or shoots were observed between *zif1-2* and Col plants when grown on MM or MM containing 30 or 60 $\mu$M Zn (data not shown). The metal content of *zifl1-1* and *zifl2-1* plants grown on MM or MM with 30 or 60 $\mu$M Zn were also determined, but no significant differences compared to the wild type were observed (data not shown).

### *zif1* Also Confers Zn Sensitivity in a Low-Zn Mutant Background

*HMA2* and *HMA4* encode Zn-transporting P-type ATPases that are important for translocation of Zn from roots to shoots (Hussain et al., 2004). *hma2 hma4* double mutants show severe Zn deficiency when grown under routine conditions in soil and have decreased shoot, but increased root, Zn content (Hussain et al., 2004). A *zif1-1 hma2-2 hma4-1* triple mutant was identified and, when grown in soil, showed an increase in shoot fresh weight compared to the *hma2-2 hma4-1* double mutant (Fig. 5, A and B), which corresponded with increased shoot Zn content of *zif1-1 hma2-2 hma4-1* compared to *hma2-2 hma4-1* (Fig. 5C). The levels of other metals were not significantly increased in the triple mutant compared with the *hma2 hma4* double mutant (data not shown).

Because the *hma2-2 hma4-1* mutants have greatly reduced shoot Zn content compared to wild type (Hussain et al., 2004), we reasoned that the triple mutant may be less sensitive to high levels of Zn compared to *zif1-1* due to decreased shoot Zn accumulation. However, when seedlings were grown on inhibitory concentrations of Zn, the *zif1-1 hma2-2 hma4-1* mutants were indistinguishable from *zif1-1* seedlings (Fig. 5, D and E) even though levels of Zn in shoots were significantly less than in the *zif1-1* seedlings (Fig. 5F). The levels of other metals were not significantly increased in *zif1-1* and *zif1-1 hma2-2 hma4-1* compared to

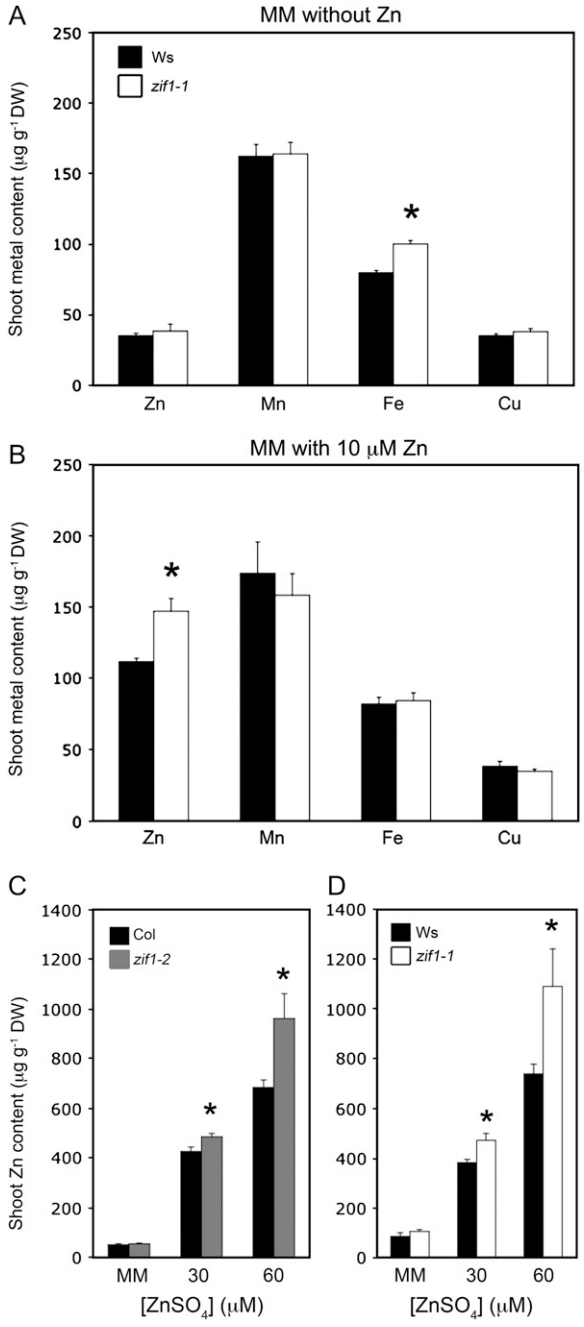


**Figure 4.** Metal accumulation in *zif1* mutants. A and B, Shoot metal content of Ws and *zif1-1* plants grown on MM without Zn (A) or MM containing 10 $\mu$M $ZnSO_4$ (B). Seven-day-old plants were transferred onto the indicated medium and grown for a further 14 d. Values are mean ± SE, and each replicate represents pooled shoots from five seedlings ($n = 8$). C, Shoot Zn content of Col and *zif1-2* plants grown on MM or MM containing 30 or 60 $\mu$M $ZnSO_4$ as described in Figure 2. Values are mean ± SE, and each replicate represents a pool of shoots from three or four seedlings ($n = 4$). D, Shoot Zn content of Ws and *zif1-1* seedlings grown on MM or MM with 30 or 60 $\mu$M $ZnSO_4$ as described in Figure 2. Values are mean ± SE, and each replicate represents a pool of shoots from five seedlings ($n = 4$). Statistical differences from wild types in A, B, C, and D were determined by *t* test (*, $P < 0.05$). Pooled tissues were collected from seedlings grown on a single plate and replicates represent separate plates.

wild type (data not shown). The increased Zn sensitivity of *zif1* and *zif1 hma2 hma4* seedlings may be due to an effect in roots. However, *zif1 hma2 hma4* mutants are expected to have a higher concentration of Zn in roots than *zif1* and so should be more Zn sensitive than the single mutant if the effect is isolated to roots. On the contrary, the shoot fresh weights of *zif1-1* and *zif1-1 hma2-2 hma4-1* are not significantly different on any Zn concentration tested (Fig. 5E). Therefore, we suggest that the Zn sensitivity of *zif1* mutants is likely to be caused by an incorrect distribution of Zn, rather than the overall increase in Zn content per se.

### *ZIF1* Shows a Broad Pattern of Expression and Is Induced in Shoots and Roots by Zn

To observe the tissue specificity of *ZIF1* expression, a 1.9-kb fragment of the *ZIF1* promoter region was fused to *uidA* ($\beta$-glucuronidase [GUS]) and transformed into Col wild-type plants. GUS expression was observed in both leaves and roots of seedlings (Fig. 6, A and B). In shoots, expression was strongest in developing leaves, whereas in older leaves expression was mostly associated with vascular tissues (Fig. 6A). A similar trend was observed in roots with strong expression in the differentiating zone of root tips, including lateral roots, but becoming restricted to vascular tissues of mature roots (Fig. 6, C and D). GUS expression was also observed in flowers, with strong expression in sepals of developing flowers, becoming confined to the sepal vasculature in mature flowers (Fig. 6, E and F), and in the vasculature of mature anthers and filaments (Fig. 6, F and G). Expression was not observed in developing anthers or anther filaments (data not shown).

To investigate whether *ZIF1* is regulated by metals, semiquantitative RT-PCR was used to measure *ZIF1* expression in plants grown on medium supplemented with subinhibitory concentrations of Zn, Cd, Mn, Fe, and Cu. *ZIF1* expression was higher in both roots and shoots of seedlings grown on medium containing 30 $\mu$M Zn or 250 $\mu$M Mn compared to seedlings grown on MM or MM with 1.5 $\mu$M Cd, 15 $\mu$M Cu, or 200 $\mu$M Fe (data not shown). To confirm the regulation of *ZIF1* by Zn and Mn, quantitative real-time RT-PCR was used to measure *ZIF1* expression in roots and shoots of seedlings grown on MM or MM with 30 $\mu$M Zn, 250 $\mu$M Mn, or 200 $\mu$M Fe. *ZIF1* expression was approximately 2-fold higher in roots of seedlings grown on Zn compared to seedlings on MM (Fig. 7A). In shoots, *ZIF1* was induced approximately 5-fold by Zn and 3-fold by Mn (Fig. 7B). Expression of *ZIF1* in seedlings grown on Fe was not significantly different from control plants (Fig. 7).

To investigate whether the concentration of Zn in growth medium affects spatial expression of *ZIF1*, GUS activity was observed in roots of *ZIF1p*-GUS seedlings grown on elevated Zn. In roots, GUS expression was higher in the vasculature of seedlings grown on Zn compared to seedlings grown on MM and expression was also observed in nonvascular cells

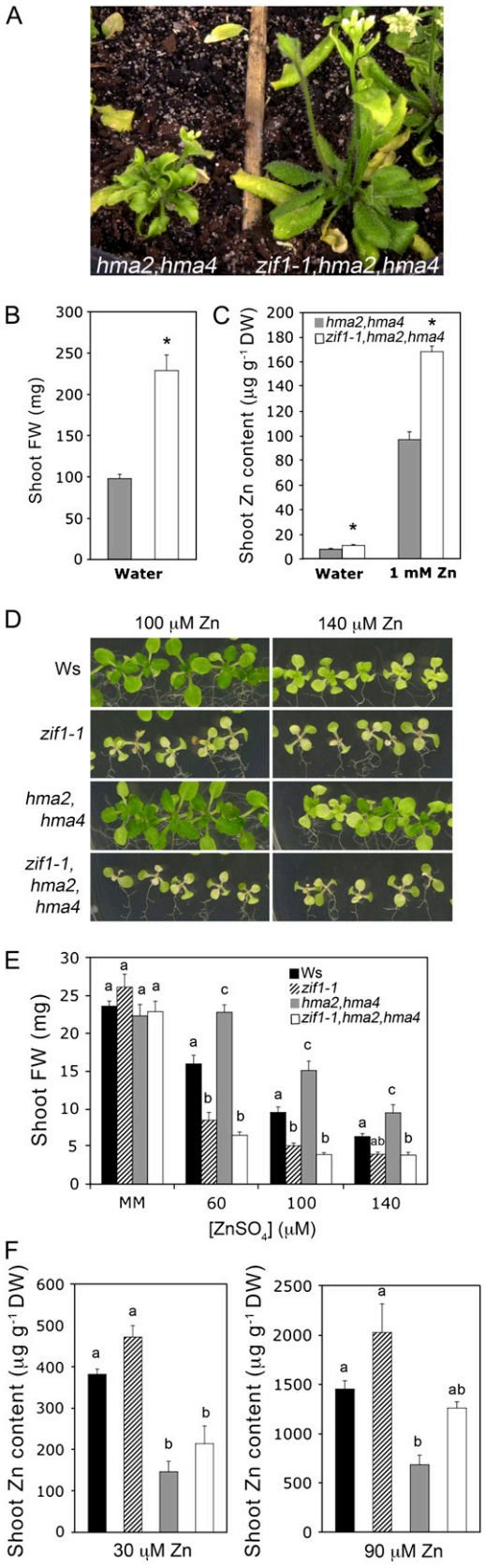


**Figure 5.** Suppression of Zn deficiency and Zn sensitivity of *zif1 hma2 hma4*. A, Forty-two-day-old *hma2-2 ham4-1* (left) and *zif1-1 hma2-2 hma4-1* plants grown in soil irrigated with water. B, Shoot fresh weight of plants shown in A (mean ± SE, $n = 8$). C, The shoot Zn content of 42-d-old *hma2-2 hma4-1* and *zif1-1 hma2-2 hma4-1* grown irrigated with water (left) or 1 mM $ZnSO_4$ (right). Each replicate is of two pooled plants (mean ± SE, $n = 8$). D, Seventeen-day-old Ws, *zif1-1*, *hma2-2 hma4-1*, and *zif1-1 hma2-2 hma4-1* plants growing on MM containing 100 or 140 μM $ZnSO_4$. E, Shoot fresh weight of plants grown as described in Figure 2 (mean ± SE, $n = 8$). F, Shoot Zn content of plants grown as described in Figure 2 on MM with 30 or 90 μM $ZnSO_4$. Each replicate is a pool of five seedlings (mean ± SE, $n = 4$). Significant differences from Ws in B and C were determined by *t* test (*, $P < 0.05$). For multiple, pairwise comparisons in E and F, significant differences between genotypes were determined for each treatment by ANOVA followed by Tukey's honestly significant difference tests. Different letters represent significantly different means within each treatment ($P < 0.05$). Pooled tissues were collected from seedlings grown on a single plate or pot and replicates represent separate plates or pots. [See online article for color version of this figure.]

(Fig. 8A). Cross-sections through the differentiated zone of roots demonstrated that, in plants grown on control medium, GUS activity was restricted to vascular and pericycle cells, whereas in the presence of 30 μM Zn, GUS activity in the vasculature and pericycle increased and was also observed in cortical cells. In the presence of the mildly inhibitory concentration of 60 μM Zn, very high GUS activity was observed in all root cells, including the epidermis (Fig. 8B). Increased *ZIF1p*-GUS expression was also observed in shoots of seedlings grown on subinhibitory concentrations of Zn. The apparent increase in expression in leaves of lines exposed to Zn was the result of persistence of expression throughout older leaves compared to the more limited, vascular expression in mature leaves of plants grown on control medium (Fig. 8C). Cross-sections through leaves showed a predominance of GUS expression in vascular cells and an absence of expression in epidermal cells in plants grown on control medium, whereas in plants grown in the presence of 30 μM Zn, GUS activity was stronger and more evenly distributed in all leaf cells (Fig. 8D).

### ZIF1 Is Localized to the Tonoplast

To determine the subcellular localization of ZIF1, a C-terminal GFP fusion was made by cloning the *ZIF* cDNA in frame with *GFP* under the control of the cauliflower mosaic virus 35S promoter and transformed into Col plants. In root tips of 35S-ZIF1-GFP lines, fluorescence localized to an internal membrane (Fig. 9A) compared to 35S-GFP controls, which fluoresced in the cytoplasm surrounding the vacuole and in nuclei (Fig. 9B). This is similar to the localization of ShMTP8-GFP (described as ShMTP1) at the tonoplast in Arabidopsis root tips (Delhaize et al., 2003; Fig. 9C). As root cells differentiated and became more highly vacuolated, the fluorescence of ZIF1-GFP began to fill the cell (Fig. 9D) and, in mature root cells, the fluorescence marked a membrane adjacent to the cell perimeter (Fig. 9E). This is consistent with ZIF1 localizing to

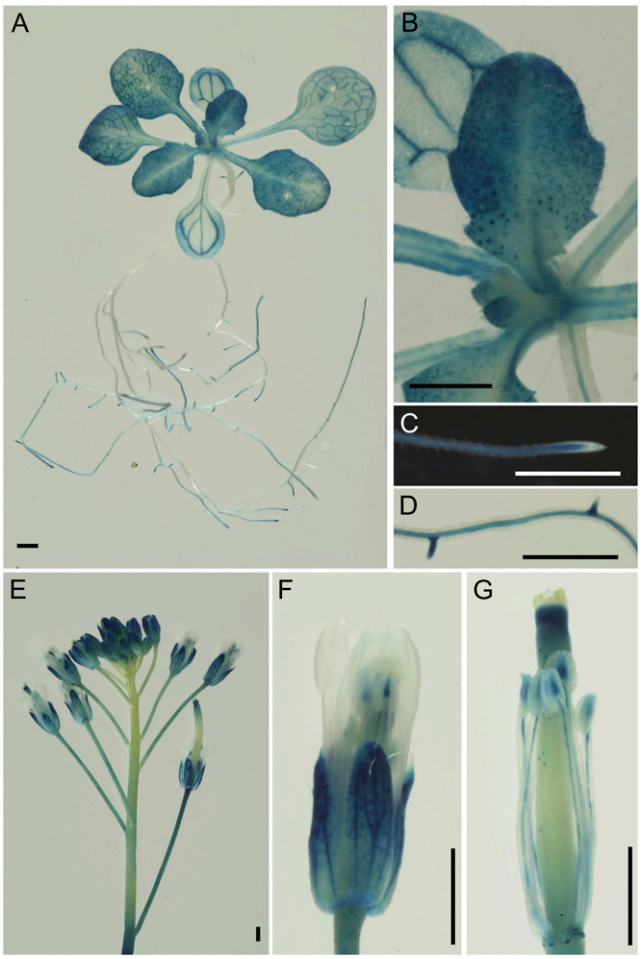


**Figure 6.** Expression of *ZIF1p*-GUS in transgenic plants. A, Fourteen-day-old seedling. B, Detail of developing leaf of seedling shown in A. C, Roots tips. D, Lateral roots. E, Inflorescences. F, Mature flower. G, Mature flower with sepals and petals removed. Bars = 1 mm.

the tonoplast of root cells. Protoplasts were also isolated from leaves of 35S-ZIF1-GFP and 35S-GFP lines. ZIF1-GFP localized to a membrane within the perimeter of the plasma membrane, made apparent by the location of the chloroplasts, which are external to the GFP-marked membrane (Fig. 9F). This is consistent with tonoplast localization of ZIF1-GFP, which is supported by 35S-GFP controls in which fluorescence fills the cytoplasm, marking the outline of the vacuole that occupies most of the cell (Fig. 9G).

To confirm that ZIF1-GFP was correctly localized, 35S-ZIF1-GFP was also transformed into the *zif1-2* mutant to test whether it could complement the Zn-sensitive phenotype. For comparison, a 35S-ZIF1 construct was also generated and transformed into *zif1-2*. Seven 35S-ZIF1 and five 35S-ZIF1-GFP independent transgenic lines were identified and two of each were selected for further analysis based on high transgene expression as determined by RT-PCR (data not shown). When tested for Zn sensitivity, these lines showed a phenotype similar to the wild type, whereas *zif1-2* lines containing the empty vector remained Zn sensitive as expected (Fig. 10, A–C). Fluorescence in *zif1-2*-complemented lines also indicated tonoplast localization of *ZIF1-GFP* (data not shown). These results indicate that overexpression of *ZIF1* or *ZIF1-GFP* complements *zif1-2*, suggesting that the ZIF1-GFP fusion is functional and correctly localized.

### Overexpression of *ZIF1* Can Confer Increased Zn Tolerance and Causes Interveinal Leaf Chlorosis

Of the four lines of *zif1-2* overexpressing *ZIF1* or *ZIF-GFP*, one showed significantly better shoot growth on medium containing 60 $\mu$M Zn, whereas a second also grew better on 120 $\mu$M Zn (Fig. 10). Of the four lines, these two had the highest levels of expression of

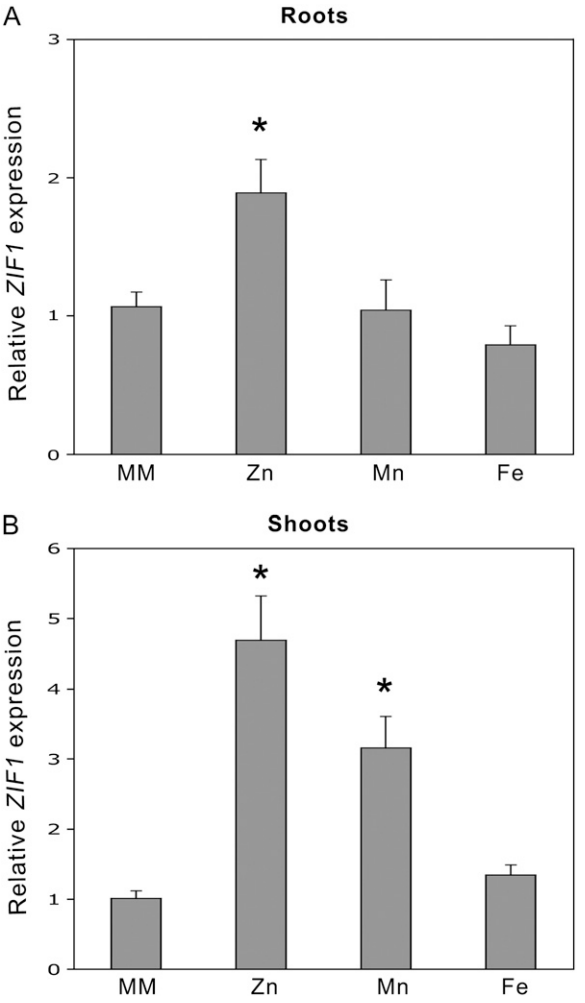


**Figure 7.** Regulation of *ZIF1* by Zn. A and B, Relative expression of *ZIF1* in roots (A) and shoots (B) of 14-d-old Col plants that had been exposed to MM or MM with 30 $\mu$M Zn, 250 $\mu$M Mn, or 200 $\mu$M Fe for 7 d. *ZIF1* and *ACT2* were amplified by real-time PCR, and expression of *ZIF1* was calculated relative to *ACT2* and normalized to mean expression in seedlings grown on MM using the $\Delta\Delta C_t$ method. Values are means ± SE ($n = 3$). Significant differences from control conditions (MM) were determined by *t* test (*, $P < 0.05$).

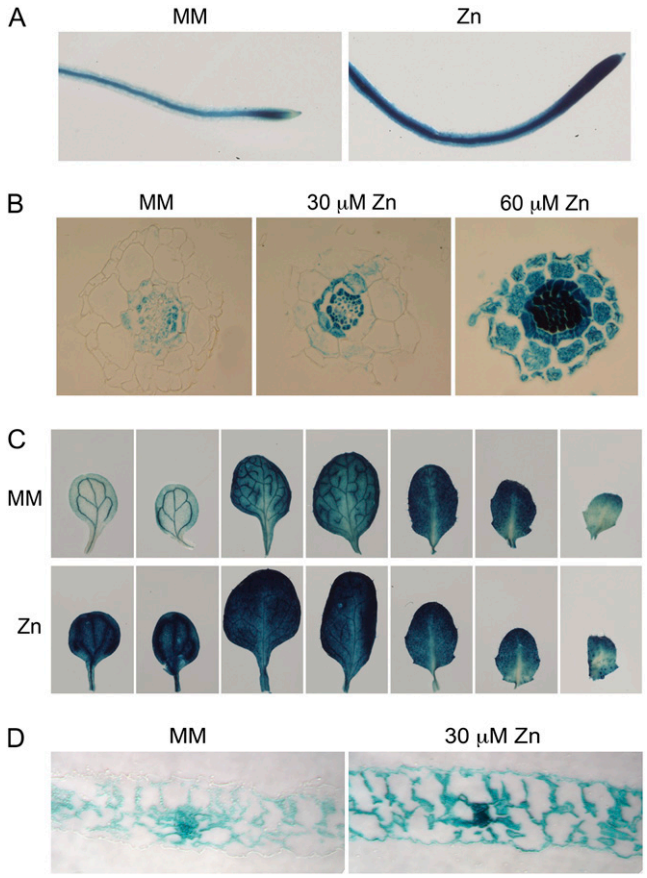


**Figure 8.** Regulation of *ZIF1p*-GUS expression by Zn. A, GUS expression in root tips of lines exposed to MM (left) or 60 $\mu$M Zn for 5 d. B, Cross-section through mature roots zone of seedlings grown on MM (left), 30 $\mu$M (middle), or 60 $\mu$M Zn (right). C, Comparison of cotyledons and leaves from seedlings exposed to MM (top) or 30 $\mu$M Zn (bottom) for 5 d. D, Cross-section through the second true leaf of seedlings exposed to MM (left) or 30 $\mu$M Zn (right).

the *ZIF1* transgene (data not shown). This indicates that overexpression of *ZIF1* from the 35S promoter can, in some circumstances, confer increased tolerance to Zn.

The *35S-ZIF1* and *35S-ZIF1-GFP* constructs and a *35S-ZIF1*-6×-His construct, which was also able to complement the Zn sensitivity of *zif1-2* (data not shown), were also transformed into Col wild-type plants. Whereas none of seven independent homozygous T3 *35S-ZIF1* lines showed *ZIF1* expression greater than in Col (data not shown), three independent homozygous 35S-ZIF1-GFP lines and two independent homozygous 35S-ZIF1-His lines with high transgene expression (Fig. 11A) were identified. When these lines were grown in soil or on agar medium for 2 to 3 weeks, leaves became chlorotic between the leaf veins, and this phenotype was also observed in *zif1-2* plants overexpressing ZIF1 (Fig. 11B).

Two lines for each construct were grown in the presence of inhibitory Zn concentrations. When tested for growth in the presence of 100 $\mu$M Zn, two of these lines showed better growth than the wild type, apparent in a significant increase in shoot fresh weight (Fig. 11C), further indicating that overexpression in some cases can confer increased Zn tolerance.

### Increased Zn Sensitivity of a *zif1 mtp1* Double Mutant

MTP1 is believed to be important for Zn tolerance in *A. thaliana* via transport of Zn into vacuoles. T-DNA mutations and RNAi knockdowns of *MTP1* confer a Zn-sensitive phenotype (Kobae et al., 2004; Desbrosses-Fonrouge et al., 2005). To investigate possible genetic interactions between *ZIF1* and *MTP1*, *zif1-1* was crossed to *mtp1-1* (Kobae et al., 2004) and a double mutant was identified from F2 progeny using PCR. Zn

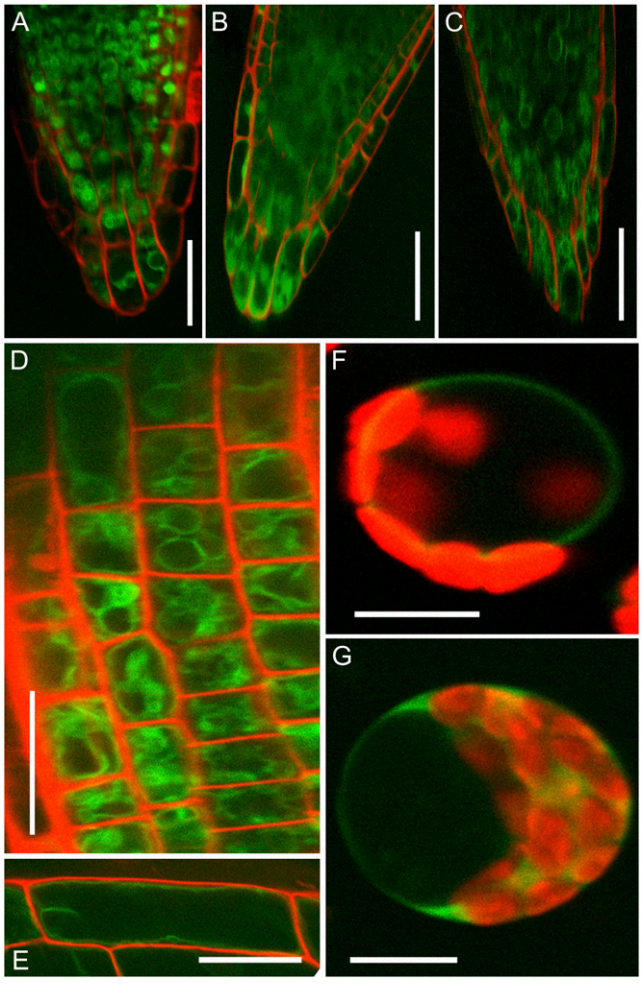


**Figure 9.** ZIF1-GFP localizes to the tonoplast. A to G, GFP fluorescence in transgenic Arabidopsis. A, ZIF1-GFP in a root tip. B, 35S-GFP in a root tip. C, ShMTP1-GFP in a root tip. D, ZIF1-GFP in differentiating root epidermal cells. E, ZIF1-GFP in a mature epidermal root cell. F, ZIF1-GFP in protoplasts isolated from leaves of stable lines. G, 35S-GFP in protoplasts isolated from leaves of stable lines. Green fluorescence indicates GFP, and red fluorescence represents cell walls stained with propidium iodide in A to E or chloroplasts in F and G. Bars = 20 $\mu$m.

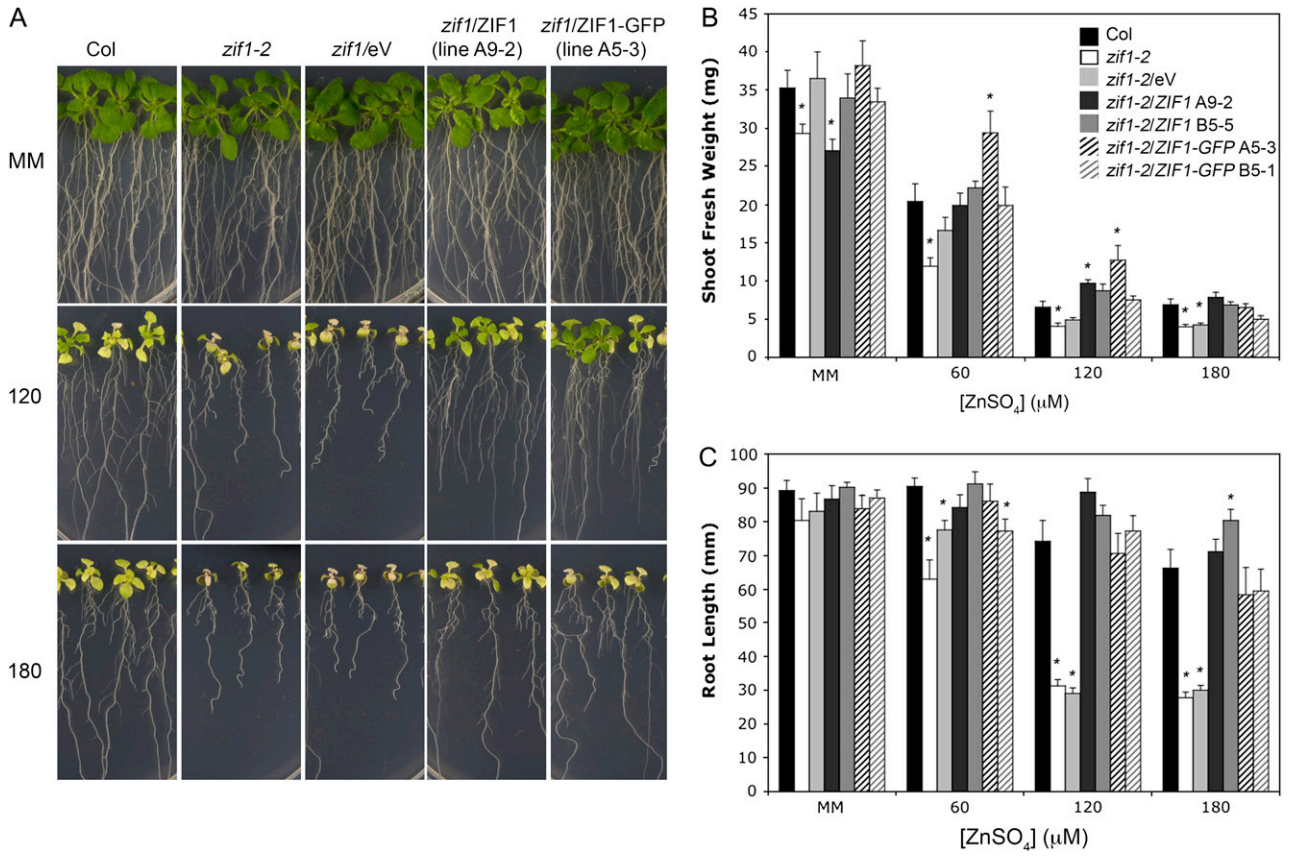


**Figure 10.** Complementation of *zif1* by overexpression of *ZIF1*. A, Seventeen-day-old transgenic lines growing vertically on MM or MM with 120 or 180 $\mu$M $ZnSO_4$. B, Shoot fresh weight. C, Root length of plants grown as described in Figure 2. Values are means ± SE ($n = 8$). Significant differences from Col were determined by *t* test (*, $P < 0.05$). [See online article for color version of this figure.]

sensitivity of the double mutant was compared to Ws wild type and the single mutants (Fig. 12). The Zn sensitivity of *mtp1-1* is less severe than that of *zif1-1* (Fig. 12A). Shoot fresh weight (Fig. 12B) and root length (Fig. 12C) were decreased to a lesser extent in *mtp1-1* than *zif1-1*, compared to Ws wild type, when grown on medium containing 60, 100, or 140 $\mu$M $ZnSO_4$. Furthermore, Zn sensitivity of the *zif1-1 mtp1-1* double mutant is more severe than *zif1-1* (Fig. 12A). When grown on 60 $\mu$M Zn, significant root growth inhibition was observed in *zif1-1 mtp1-1*, whereas the root length of *zif1-1* was not significantly different from Ws (Fig. 12C). In addition, the difference in root length between *zif1-1* and *zif1-1 mtp1-1* was also visible on 100 $\mu$M Zn (Fig. 12A). This observation implies that *ZIF1* and *MTP1* contribute to Zn tolerance in *A. thaliana* via independent mechanisms.

## DISCUSSION

Three alleles of a novel Zn-sensitive mutant of *A. thaliana* have been identified. When grown on medium containing inhibitory concentrations of Zn, mutants showed as much as a 50% reduction in fresh weight compared to wild-type plants. Increased sensitivity to other essential metals was not observed, although they showed increased sensitivity and tolerance, respectively, for Cd and Ni, which are nonessential elements in Arabidopsis. In *zif1* mutants, levels of Zn, but not of other metals, were consistently increased. This was observed in the *zif1* mutants themselves and also in the effect of *zif1* in the Zn-deficient *hma2 hma4* background. *ZIF1* was also strongly induced by subinhibitory concentrations of Zn and, to a lesser extent, Mn, but not other metals. Together, these observations suggest that the function of ZIF1 is relatively specific to Zn homeostasis.

Localization of a ZIF1-GFP fusion to the tonoplast suggests that ZIF1 may affect the distribution of Zn between the vacuole and the tonoplast. Because mutants are Zn sensitive, it seems likely that loss of ZIF1 leads to an accumulation of Zn in the cytosol. However, if Zn is accumulating in the cytosol of *zif1*, the overall increased Zn content per unit dry weight in these plants is difficult to explain. MTP1 and MTP3 in Arabidopsis are, like ZIF1, localized to the tonoplast and are believed to transport Zn into vacuoles. RNAi-mediated knockdown of *MTP1* or *MTP3* also confers Zn sensitivity (Desbrosses-Fonrouge et al., 2005; Arrivault et al., 2006). In contrast to the observations

for *zif1*, *MTP1* knockdown led to a decrease in Zn in leaves when grown in soil, although the Zn content of these lines when grown on higher Zn concentrations has not been reported. *MTP3* knockdown lines had increased leaf Zn content when grown on soil or on medium containing 30 $\mu$M Zn, similar to *zif1*, and it was proposed that this was due to decreased sequestration of Zn in root vacuoles, although Zn content in roots of these lines was not reported. The increased shoot Zn content of *zif1* may be due, at least in part, to decreased Zn sequestration in roots, and this may also explain the increased shoot Zn content of soil-grown *zif1-1 hma2-2 hma4-1* compared to *hma2-2 hma4-1*. Notwithstanding that *ZIF1* is expressed in most tissues in plants exposed to high levels of Zn, it is also possible that loss of ZIF1 function may lead to redistribution of Zn in shoot tissues.

The *mtp1-1* T-DNA mutant is Zn sensitive (Kobae et al., 2004). The Zn-sensitive phenotype of *zif1-1* mutants is more severe than *mtp1-1* and a *zif1-1 mtp1-1* double mutant is more Zn sensitive than *zif1-1*. This

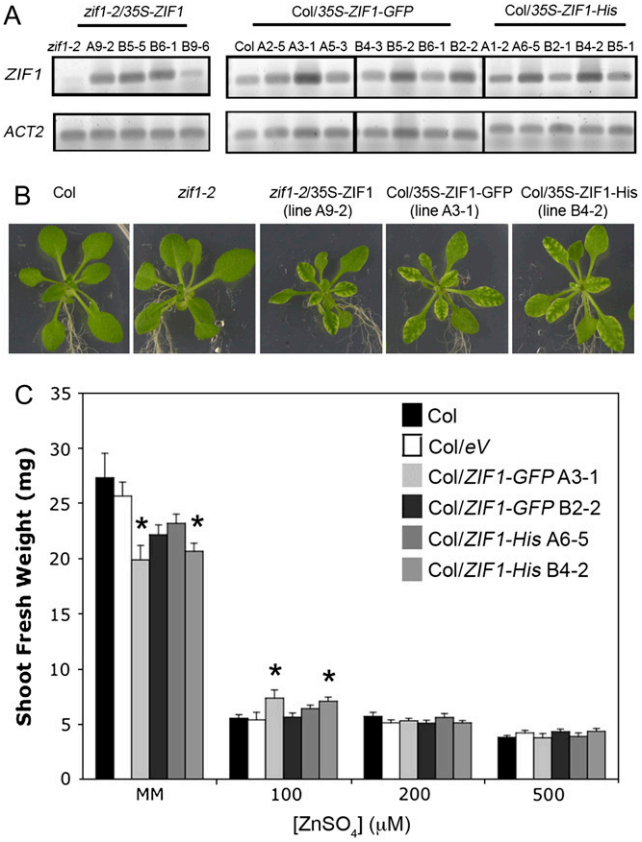


**Figure 11.** Interveinal chlorosis of *35S-ZIF1* transgenic lines. A, RT-PCR of Col, *zif1-2*, and transgenic lines expressing *35S-ZIF1*, *35S-ZIF1-GFP*, or *35S-ZIF1-His*. *ZIF1* (22 cycles) and *ACT2* (18 cycles) were amplified from cDNA made from pooled, whole 10-d-old seedlings. Gels were stained with SYBR Green I. B, Twenty-one-day-old plants growing on MM. C, Shoot fresh weight of plants grown as described in Figure 2. Values are means ± SE ($n = 8$). Statistical differences were determined compared to Col by *t* test (*, $P < 0.05$). [See online article for color version of this figure.]

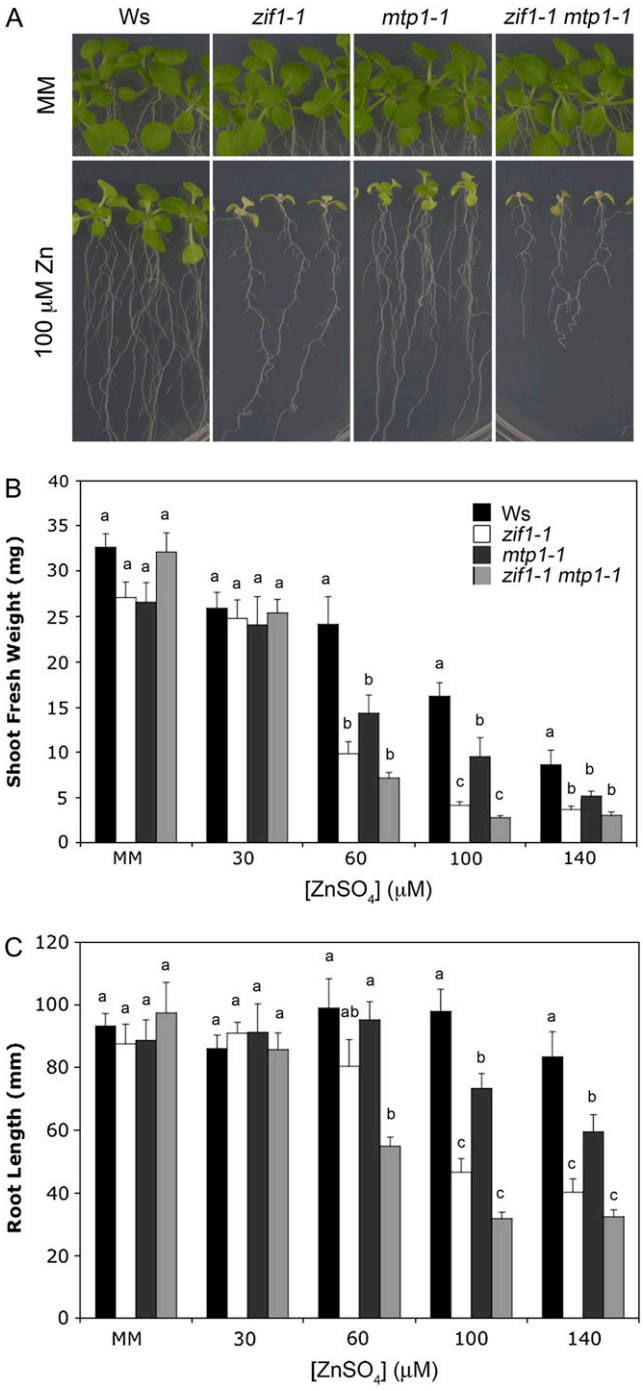


**Figure 12.** Zn hypersensitivity of *zif1 mtp1* double mutants. A, Seventeen-day-old Ws, *zif1-1*, *mtp1-1*, and *zif1-1 mtp1-1* plants growing vertically on MM or MM containing 100 $\mu$M $ZnSO_4$. B, Shoot fresh weight. C, Root length of plants grown as described in Figure 2. Values are mean ± SE ($n = 8$). For multiple, pairwise comparisons, significant differences between genotypes were determined for each treatment by ANOVA followed by Tukey's honestly significant difference tests. Different letters represent significantly different means within each treatment ($P < 0.05$). [See online article for color version of this figure.]

suggests that ZIF1 and MTP1 contribute to Zn tolerance via independent mechanisms. If ZIF1 and MTP1 function in the same pathway of vacuolar Zn sequestration, the double mutant would be expected to be as sensitive to Zn as the *zif1* single mutant. Unlike the constitutively expressed *MTP1* (van der Zaal et al., 1999), *ZIF1* is highly induced in plants exposed to increased, but noninhibitory, Zn concentrations, suggesting ZIF1 may constitute an MTP1-independent, inducible pathway for vacuolar Zn sequestration. Indeed, GUS expression results indicating that *ZIF1* is expressed in most cells in the plant under conditions of high Zn exposure imply an important role for ZIF1 in Zn tolerance in *A. thaliana*.

In view of the apparent role of ZIF1 in Zn tolerance and because most of the MFS proteins for which the substrate is known transport organic molecules, it is possible that ZIF1 transports a Zn ligand. Nicotianamine, phytochelatin, and His have been implicated as metal-binding ligands in plants (Callahan et al., 2006), but these are not likely to be important Zn-binding ligands in vacuoles. Organic acids, such as citrate and malate, have been implicated in Zn homeostasis as ligands in plant vacuoles and are therefore good candidates for the ZIF1 substrate. Computer modeling of the likely Zn ligands in vacuoles of tobacco (*Nicotiana tabacum*) suggested >90% should be bound to citrate (Wang et al., 1992). In *T. caerulescens*, x-ray absorption spectroscopy analysis indicated Zn citrate is the predominant species in shoots (Salt et al., 1999), whereas extended x-ray absorption spectroscopy in *A. halleri* suggested that malate is the most likely Zn ligand in leaves (Sarret et al., 2002). Some tonoplast citrate or malate transporters have been identified, but none is an MFS protein. AttDT in *A. thaliana* transports malate into vacuoles (Emmerlich et al., 2003) and a vacuolar citrate transporter, CsCit1, identified in navel orange (*Citrus sinensis* cv Washington) based on similarity to *AttDT*, transported citrate out of yeast tonoplast vesicles by proton symport (Shimada et al., 2006). A transporter that mediates uptake of citrate into plant vacuoles, which is believed to occur via citrate-$H^+$ antiport (Oleski et al., 1987; Rentsch and Martinoia, 1991), is yet to be identified. Given that ZIF1 is most similar to MFS proteins that transport by substrate-$H^+$ antiport and contains protein sequence motifs conserved among these members of the MFS, ZIF1 may fulfill this role in *A. thaliana*.

A second model is that ZIF1 transports a Zn chelate and functions in addition to a tonoplast carrier for the free ligand. This model has a precedent because, although MFS proteins are not known to transport metal ions, some transport metal-ligand complexes. The tetracycline resistance protein from *E. coli*, TetA(B), which is a member of the drug-$H^+$ antiporter family, transports a divalent metal-tetracycline complex in exchange for protons (Yamaguchi et al., 1990, 1991), and the siderophore transporter family of MFS proteins is involved in uptake of Fe-siderophores in yeast and fungi (Heymann et al., 1999, 2000a, 2000b; Yun et al., 2000a, 2000b; Ardon et al., 2001; Haas et al., 2003). The indication that ZIF1 functions independently of MTP1 also supports a model in which the substrate is a Zn chelate, whereby a separate $Zn^{2+}$ transporter is not required. However, it may be that ZIF1 function is dependent on a vacuolar $Zn^{2+}$ transporter other than MTP1. Overexpression of *ZIF1* could, in some transgenic lines, confer a significant increase in growth in the presence of inhibitory concentrations of Zn. The absence of Zn tolerance in all overexpression lines is probably because expression of endogenous *ZIF1* is normally high in these conditions. Nevertheless, this may argue in favor of the second model, where overexpression of a protein transporting a Zn ligand bound to Zn might more readily confer increased tolerance because its function would be independent of a separate mechanism transporting Zn itself into the vacuole. The interveinal chlorosis in 35S-ZIF1 transgenic lines may be caused by a cytosolic deficiency of the ZIF1 substrate, whether that is Zn, an organic acid, or both. The pattern of bleaching in these lines is reciprocal to *ZIF1p*-GUS expression in transgenic plants grown on MM, suggesting that the phenotype may be a result of high expression of ZIF1 in cells where it is not normally expressed.

In addition to Zn, *zif1* mutants or *ZIF1* expression also showed effects in the presence of excess Cd, Ni, or Mn. That *zif1* mutants are also Cd sensitive may be because Zn and Cd share chemical similarities and are often associated in biological systems, such as in Zn-Cd hyperaccumulators. The candidate Zn ligand, citrate, is also predicted by computer simulation to be the predominant ligand for Cd in tobacco vacuoles (Wang et al., 1991). Ni citrate has also been implicated in Ni tolerance and Ni hyperaccumulation (Kramer et al., 2000). Whereas experiments investigating the mechanism of ion transport into oat (*Avena sativa*) root tonoplast vesicles indicated that Zn and Cd are transported into vacuoles via proton antiport (Salt and Wagner, 1993; Gonzalez et al., 1999), $Ni^{2+}$-$H^+$ antiport or nucleotide-dependent Ni transport could not be demonstrated and the evidence suggested a slower association of Ni with the tonoplast rather than transport across the membrane (Gries and Wagner, 1998). Studies using the Ni hyperaccumulator *Thlaspi goesingense* and the related nonaccumulator *Thlaspi arvense* suggest that up to 75% of symplastic Ni in the hyperaccumulator and 25% in the nonaccumulator are associated with the vacuolar fraction of shoot tissue (Kramer et al., 2000). However, the subcellular fractionation technique used would not have distinguished between tonoplast-associated Ni and Ni localized within the vacuolar lumen. Moreover, this result also implies that, at least in the nonaccumulator species, a large proportion of Ni remains in the cytosol, presumably bound by ligands, without causing toxicity. If the *ZIF1* substrate is accumulating in the cytosol of *zif1* mutants and has sufficient affinity to sequester excess Ni at cytosolic pH, these plants may show increased Ni tolerance. This would also imply that the ZIF1

substrate is not able to effectively chelate Zn or Cd in the cytosol. Alternatively, the Ni tolerance observed in *zif1* mutants may be an indirect effect due to increased accumulation of Zn in the cytosol. The response of *ZIF1* in plants exposed to increased Mn suggests a possible role for ZIF1 in Mn tolerance. Although the vacuole is the major store for Mn (Pittman, 2005), Mn sensitivity was not observed in *zif1* mutants, suggesting that the effect of Mn on *ZIF1* expression may be indirect.

It remains unclear whether *AtZIFL1*, *AtZIFL2*, and the putative plant orthologs are likely to have functions similar to or divergent from *ZIF1*. Although *ZIFL1* and *ZIFL2* do not appear to contribute to Zn tolerance at the level of the whole plant, they may have similar substrate specificities but function at different membranes or in different cell types. The only indication of function for the plant orthologs is the identification of *Zm-mfs1* as a transcript that is induced by a range of defense-related conditions, including fungal pathogen infection (Simmons et al., 2003). It may be that the maize ortholog has a function divergent from *ZIF1*; however, there is mounting evidence for a relationship between metal accumulation and pathogen resistance (Boyd, 2004; Hanson et al., 2004; Dellagi et al., 2005; Jiang et al., 2005; Mirouze et al., 2006; Poschenrieder et al., 2006), presenting the possibility that the biochemical functions of Zm-mfs1 and ZIF1 may be similar even though the physiological roles have diverged.

In summary, we suggest that ZIF1 plays an important role in Zn tolerance in *A. thaliana* by participating in vacuolar sequestration of Zn. Because many MFS proteins transport organic molecules, the function of ZIF1 may be to transport the primary Zn ligand across the tonoplast. In the plant species studied, this ligand is likely to be an organic acid, most commonly citrate. However, definitive evidence for the identity of this molecule in plants remains elusive. Further characterization of ZIF1 and the putative plant orthologs should provide insight into the identity of the Zn ligand in vacuoles and its importance for Zn tolerance in a range of plant species.

## MATERIALS AND METHODS

### Plant Materials and Growth Conditions

Arabidopsis (*Arabidopsis thaliana*) plants were grown in soil and agar as previously described (Howden et al., 1995). MM comprised 5 mM $KNO_3$, 2.5 mM $KH_2PO_4$, 2 mM $MgSO_4$, 2 mM $Ca(NO_3)_2$, 70 $\mu$M $H_3BO_3$, 50 $\mu$M Fe(III)-EDTA, 14 $\mu$M $MnSO_4$, 10 $\mu$M NaCl, 1 $\mu$M $ZnSO_4$, 0.5 $\mu$M $CuSO_4$, 0.2 $\mu$M $(NH_4)_6Mo_7O_{24}$, and 0.01 $\mu$M $CoCl_2$ (pH 5.8) with 2% (w/v) Suc and 0.8% to 1.0% Bacto agar for solid medium. For metal-sensitivity experiments, 7-d-old seedlings were transferred from MM to MM plates containing the indicated concentration of metal. Four plants of two genotypes were grown on each plate and each genotype was grown on two plates for each condition, providing eight individuals of each genotype for each condition. Plates were grown vertically for an additional 10 d and shoot fresh weight and root length or root fresh weight were determined.

The *zif1-1* mutant was identified from a T-DNA line generated in the Ws ecotype (Krysan et al., 1999) and the location of the insertion was determined using inverse PCR and nucleotide sequencing. T-DNA mutants in Col were identified using the SIGnAL Web site (http://signal.salk.edu) and ordered through the Arabidopsis Biological Resource Center (ABRC; Alonso et al., 2003). The location of the insertions was confirmed by nucleotide sequencing of PCR products amplified using a left-border primer and primers specific to the gene. All lines were backcrossed to the wild type, and homozygous mutant lines were identified from F2 populations by PCR using gene-specific primers that flank the T-DNA for the wild-type allele or the left-border primer and a gene-specific primer for the mutant allele. The *zif1-3* allele was identified by screening EMS-mutagenized Col-0 M2 seed (Lehle Seeds) on MM containing 100 $\mu$M Zn. M3 plants were backcrossed to Col-0 and, after confirming 3:1 segregation of the phenotype in F2, a homozygous F3 population was identified, which was crossed to *zif1-2* for complementation. Nucleotide sequencing of the putative exons of *zif1-3* indicated a single base pair substitution of G to A at position 1,414 of the predicted cDNA. Primers are described in Supplemental Table S1.

### RT-PCR Techniques

Total RNA was extracted using the RNAqueous RNA extraction kit (Ambion). To determine gene expression in mutants and transgenics, 30 mg of tissue pooled from 8-d-old seedlings were used. To determine *ZIF1* metal regulation, roots or shoots from four 14-d-old seedlings were pooled. RNA was DNAse treated using the DNA-free kit (Ambion) and cDNA was made from 5 $\mu$g of RNA using the SuperScript first-strand cDNA synthesis system (Invitrogen). PCR was performed using the primer sets indicated. For semi-quantitative PCR, gels were stained with SYBR Green I (Invitrogen) and scanned using a Typhoon 8600 variable mode imager (Molecular Dynamics) in fluorescence acquisition mode using a fluorescein emission filter. The intensity of bands was quantified using ImageQuant software (Molecular Dynamics). For quantitative real-time PCR, cDNA was synthesized from 2 $\mu$g of DNAse-treated RNA, extracted from leaves from three seedlings or roots from six seedlings, and real-time PCR was performed in duplicate on 20 ng of cDNA using the platinum SYBR Green qPCR SuperMix UDG (Invitrogen) with primers at a concentration of 200 nM on a Rotor-Gene 3000 (Corbett Research). Primer efficiencies were determined and relative expression of *ZIF1* was calculated using the $\Delta\Delta C_t$ method by normalizing to *ACT2* expression.

### Measurement of Metal Content in Plant Tissues

Metal content of plant tissue was determined as described previously (Hussain et al., 2004). Briefly, plant tissues were harvested and oven dried at 70°C for 4 d. Weighed samples were digested in 70% $HNO_3$ overnight at room temperature, then at 80°C for 2 h. Digested samples were diluted to a final concentration of 7% $HNO_3$ with deionized water and metals were measured using a Vista-AX ICP-AES (Varian).

### *ZIF1p*-GUS Fusion Construct Lines

The upstream region of *ZIF1* from −1,991 to +84 was amplified by PCR from Col genomic DNA using primers designed to include an upstream *Sal*I site and a downstream *Spe*I site. This fragment, which spans the entire intergenic region and encodes approximately 1.9 kb of the promoter region to the adjacent gene and the first 28 codons of ZIF1, was ligated into the *Sal*I and *Xba*I sites of pBI101 (CLONTECH) so that the ATG of *ZIF1* was in frame with the GUS gene. Primers are described in Supplemental Table S1. The *ZIF1p*-GUS construct was transformed into Col plants by the Agrobacterium-mediated floral-dip method (Clough and Bent, 1998). A total of eight independent homozygous T3 lines were identified that segregated 3:1 kanamycin resistance in T2 generations. Histochemical staining of transgenic lines was carried out according to Jefferson et al. (1987). Six of the eight lines showed the same GUS expression pattern and two representative lines were selected for detailed analysis. For sections, stained tissues were imbedded in paraffin essentially as described previously (Johnson et al., 2002) and 8-$\mu$m sections were made.

### *35S-ZIF1*, *35S-ZIF1-GFP*, and *35S-ZIF1-His* Construct Lines

The open reading frame of *ZIF1* was amplified by PCR from Col cDNA using an upstream primer that included a *Sal*I site immediately preceding the

ATG and alternative downstream primers, both including a *Spe*I site that spanned the final codon and either maintained the TGA stop codon for *35S-ZIF1* or omitted the stop for *35S-ZIF1-GFP*. For *35S-ZIF1*, the fragment was ligated into the *Xho*I and *Xba*I sites of *35S-GFP-JFH1* (Hong et al., 1999), replacing GFP. For *35S-ZIF1-GFP*, the fragment was ligated into the *Xho*I and *Spe*I sites, in frame with GFP. The *35S-ZIF1-His* construct was generated by ligating an adapter duplex, designed to include *Spe*I and *Bam*HI sites, which flank a 6×-His epitope sequence, into the *Spe*I and *Bam*HI sites of *35S-ZIF1-GFP*. Primers are described in Supplemental Table S1. Constructs were transformed into Col wild-type and *zif1-2* plants by the Agrobacterium-mediated floral-dip method (Clough and Bent, 1998) and homozygous T3 populations were identified from T2 populations segregating 3:1 BASTA (glufosinate-ammonium) resistance. Eight *35S-ZIF1*, 10 *35S-ZIF1-GFP*, and five *35S-ZIF1-His* independent transgenic lines were identified in the Col background and six independent lines were identified for each construct in *zif1-2*. Fluorescence images were captured by laser-scanning confocal microscopy with an Olympus BX60 microscope connected to an Optiscan F900E master control unit using tetramethylrhodamine isothiocyanate and fluorescein isothiocyanate filters simultaneously. The *35S-GFP* and *35S-ShMTP1-GFP* control lines used for imaging were described previously (Delhaize et al., 2003).

The AGI locus identifiers are as follows: *ZIF1*, At5g13740; *ZIFL1*, At5g13750; and *ZIFL2*, At3g43790. The DNA sequences can be found in the GenBank data libraries: *ZIF1*, NM_121377; *ZIFL1*, NM_180705; and *ZIFL2*, NM_114247. The accession numbers of insertion mutants are: *zif1-2*, SALK_011408; *zifl2-1*, SALK_030690; and *zifl2-1*, SALK_059042.

## Supplemental Data

The following materials are available in the online version of this article.

**Supplemental Table S1.** List of primers.

## ACKNOWLEDGMENTS

We wish to thank Professor Alan Baker and Dr. Scott Laidlaw for access to ICP-AES, Bruce Abaloz for embedding and sectioning, Dr. Manny Delhaize for providing 35S-GFP and 35S-ShMTP8-GFP transgenic lines, Professor Masayoshi Maeshima for providing *mtp1-1* seeds, and Quentin Lang for photography. We thank the Australian Research Council for support.

Received October 26, 2006; accepted January 28, 2007; published February 2, 2007.

## LITERATURE CITED

**Alonso JM, Stepanova AN, Leisse TJ, Kim CJ, Chen HM, Shinn P, Stevenson DK, Zimmerman J, Barajas P, Cheuk R, et al** (2003) Genome-wide insertional mutagenesis of *Arabidopsis thaliana*. Science **301:** 653–657

**Ardon O, Bussey H, Philpott C, Ward DM, Davis-Kaplan S, Verroneau S, Jiang B, Kaplan J** (2001) Identification of a *Candida albicans* ferrichrome transporter and its characterization by expression in *Saccharomyces cerevisiae*. J Biol Chem **276:** 43049–43055

**Arrivault S, Senger T, Kramer U** (2006) The Arabidopsis metal tolerance protein AtMTP3 maintains metal homeostasis by mediating Zn exclusion from the shoot under Fe deficiency and Zn oversupply. Plant J **46:** 861–879

**Axelsen KB, Palmgren MG** (2001) Inventory of the superfamily of P-type ion pumps in Arabidopsis. Plant Physiol **126:** 696–706

**Baxter I, Tchieu J, Sussman MR, Boutry M, Palmgren MG, Gribskov M, Harper JF, Axelsen KB** (2003) Genomic comparison of P-type ATPase ion pumps in Arabidopsis and rice. Plant Physiol **132:** 618–628

**Becher M, Talke IN, Krall L, Kramer U** (2004) Cross-species microarray transcript profiling reveals high constitutive expression of metal homeostasis genes in shoots of the zinc hyperaccumulator *Arabidopsis halleri*. Plant J **37:** 251–268

**Berg JM, Shi Y** (1996) The galvanization of biology: a growing appreciation for the roles of zinc. Science **271:** 1081–1085

**Bloss T, Clemens S, Nies D** (2002) Characterization of the ZAT1p zinc transporter from *Arabidopsis thaliana* in microbial model organisms and reconstituted proteoliposomes. Planta **214:** 783–791

**Boyd RS** (2004) Ecology of metal hyperaccumulation. New Phytol **162:** 563–567

**Callahan DL, Baker AJM, Kolev SD, Wedd AG** (2006) Metal ion ligands in hyperaccumulating plants. J Biol Inorg Chem **11:** 2–12

**Clemens S** (2001) Molecular mechanisms of plant metal tolerance and homeostasis. Planta **212:** 475–486

**Clough SJ, Bent AF** (1998) Floral dip: a simplified method for Agrobacterium-mediated transformation of *Arabidopsis thaliana*. Plant J **16:** 735–743

**Cobbett CS, Hussain D, Haydon MJ** (2003) Structural and functional relationships between type 1(B) heavy metal-transporting P-type ATPases in Arabidopsis. New Phytol **159:** 315–321

**Delhaize E, Kataoka T, Hebb DM, White RG, Ryan PR** (2003) Genes encoding proteins of the cation diffusion facilitator family that confer manganese tolerance. Plant Cell **15:** 1131–1142

**Dellagi A, Rigault M, Segond D, Roux C, Kraepiel Y, Cellier F, Briat J-F, Gaymard F, Expert D** (2005) Siderophore-mediated upregulation of Arabidopsis ferritin expression in response to *Erwinia chrysanthemi* infection. Plant J **43:** 262–272

**Desbrosses-Fonrouge A-G, Voigt K, Schroder A, Arrivault S, Thomine S, Kramer U** (2005) *Arabidopsis thaliana* MTP1 is a Zn transporter in the vacuolar membrane which mediates Zn detoxification and drives leaf Zn accumulation. FEBS Lett **579:** 4165–4174

**Drager DB, Desbrosses-Fonrouge AG, Krach C, Chardonnens AN, Meyer RC, Saumitou-Laprade P, Kramer U** (2004) Two genes encoding *Arabidopsis halleri* MTP1 metal transport proteins co-segregate with zinc tolerance and account for high *MTP1* transcript levels. Plant J **39:** 425–439

**Elbaz B, Shoshani-Knaani N, David-Assael O, Mizrachy-Dagri T, Mizrahi K, Saul H, Brook E, Berezin I, Shaul O** (2006) High expression in leaves of the zinc hyperaccumulator *Arabidopsis halleri* of Ah*MHX*, a homolog of an *Arabidopsis thaliana* vacuolar metal/proton exchanger. Plant Cell Environ **29:** 1179–1190

**Emmerlich V, Linka N, Reinhold T, Hurth MA, Traub M, Martinoia E, Neuhaus HE** (2003) The plant homolog to the human sodium/dicarboxylic cotransporter is the vacuolar malate carrier. Proc Natl Acad Sci USA **100:** 11122–11126

**Eren E, Arguello JM** (2004) Arabidopsis HMA2, a divalent heavy metal-transporting PIB-type ATPase, is involved in cytoplasmic $Zn^{2+}$ homeostasis. Plant Physiol **136:** 3712–3723

**Gaither LA, Eide DJ** (2001) Eukaryotic zinc transporters and their regulation. Biometals **14:** 251–270

**Gonzalez A, Koren'Kov V, Wagner GJ** (1999) A comparison of Zn, Mn, Cd, and Ca transport mechanisms in oat root tonoplast vesicles. Physiol Plant **106:** 203–209

**Gravot A, Lieutaud A, Verret F, Auroy P, Vavasseur A, Richaud P** (2004) AtHMA3, a plant P-1B-ATPase, functions as a Cd/Pb transporter in yeast. FEBS Lett **561:** 22–28

**Gries GE, Wagner GJ** (1998) Association of nickel versus transport of cadmium and calcium in tonoplast vesicles of oat roots. Planta **204:** 390–396

**Grotz N, Fox T, Connolly E, Park W, Guerinot ML, Eide D** (1998) Identification of a family of zinc transporter genes from Arabidopsis that respond to zinc deficiency. Proc Natl Acad Sci USA **95:** 7220–7224

**Haas H, Schoeser M, Lesuisse E, Ernst JF, Parson W, Abt B, Winkelmann G, Oberegger H** (2003) Characterization of the *Aspergillus nidulans* transporters for the siderophores enterobactin and triacetylfusarinine C. Biochem J **371:** 505–513

**Hammond JP, Bowen HC, White PJ, Mills V, Pyke KA, Baker AJM, Whiting SN, May ST, Broadley MR** (2006) A comparison of the *Thlaspi caerulescens* and *Thlaspi arvense* shoot transcriptomes. New Phytol **170:** 239–260

**Hanson B, Lindblom SD, Loeffler ML, Pilon-Smits EAH** (2004) Selenium protects plants from phloem-feeding aphids due to both deterrence and toxicity. New Phytol **162:** 655–662

**Heymann P, Ernst JF, Winkelmann G** (1999) Identification of a fungal triacetylfusarinine C siderophore transport gene (*TAF1*) in *Saccharomyces cerevisiae* as a member of the major facilitator superfamily. Biometals **12:** 301–306

**Heymann P, Ernst JF, Winkelmann G** (2000a) A gene of the major facilitator

superfamily encodes a transporter for enterobactin (Enb1p) in *Saccharomyces cerevisiae.* Biometals **13:** 65–72

**Heymann P, Ernst JF, Winkelmann G** (2000b) Identification and substrate specificity of a ferrichrome-type siderophore transporter (Arn1p) in *Saccharomyces cerevisiae.* FEMS Microbiol Lett **186:** 221–227

**Hong BM, Ichida A, Wang YW, Gens JS, Pickard BC, Harper JF** (1999) Identification of a calmodulin-regulated $Ca^{2+}$-ATPase in the endoplasmic reticulum. Plant Physiol **119:** 1165–1175

**Howden R, Goldsbrough PB, Andersen CR, Cobbett CS** (1995) Cadmium-sensitive, *cad1* mutants of *Arabidopsis thaliana* are phytochelatin deficient. Plant Physiol **107:** 1059–1066

**Hussain D, Haydon MJ, Wang Y, Wong E, Sherson SM, Young J, Camakaris J, Harper JF, Cobbett CS** (2004) P-type ATPase heavy metal transporters with roles in essential zinc homeostasis in Arabidopsis. Plant Cell **16:** 1327–1339

**Ishimaru Y, Suzuki M, Kobayashi T, Takahashi M, Nakanishi H, Mori S, Nishizawa NK** (2005) OsZIP4, a novel zinc-regulated zinc transporter in rice. J Exp Bot **56:** 3207–3214

**Jefferson RA, Kavanagh TA, Bevan MW** (1987) Gus fusions—beta-glucuronidase as a sensitive and versatile gene fusion marker in higher plants. EMBO J **6:** 3901–3907

**Jiang RF, Ma DY, Zhao FJ, McGrath SP** (2005) Cadmium hyperaccumulation protects *Thlaspi caerulescens* from leaf feeding damage by thrips (*Frankliniella occidentalis*). New Phytol **167:** 805–814

**Johnson CS, Kolevski B, Smyth DR** (2002) *TRANSPARENT TESTA GLABRA2,* a trichome and seed coat development gene of Arabidopsis, encodes a WRKY transcription factor. Plant Cell **14:** 1359–1375

**Kobae Y, Uemura T, Sato MH, Ohnishi M, Mimura T, Nakagawa T, Maeshima M** (2004) Zinc transporter of Arabidopsis thaliana AtMTP1 is localized to vacuolar membranes and implicated in zinc homeostasis. Plant Cell Physiol **45:** 1749–1758

**Kramer U, Pickering IJ, Prince RC, Raskin I, Salt DE** (2000) Subcellular localization and speciation of nickel in hyperaccumulator and non-accumulator Thlaspi species. Plant Physiol **122:** 1343–1354

**Krysan PJ, Young JC, Sussman MR** (1999) T-DNA as an insertional mutagen in Arabidopsis. Plant Cell **11:** 2283–2290

**Lopez-Millan AF, Ellis DR, Grusak MA** (2004) Identification and characterization of several new members of the ZIP family of metal ion transporters in *Medicago truncatula.* Plant Mol Biol **54:** 583–596

**Mills RF, Krijger GC, Baccarini PJ, Hall JL, Williams LE** (2003) Functional expression of AtHMA4, a P-1B-type ATPase of the Zn/Co/Cd/Pb subclass. Plant J **35:** 164–176

**Mirouze M, Sels J, Richard O, Czernic P, Loubet S, Jacquier A, Francois I, Cammue BPA, Lebrun M, Berthomieu P, et al** (2006) A putative novel role for plant defensins: a defensin from the zinc hyper-accumulating plant, *Arabidopsis halleri,* confers zinc tolerance. Plant J **47:** 329–342

**Moreau S, Thomson RM, Kaiser BN, Trevaskis B, Guerinot ML, Udvardi MK, Puppo A, Day DA** (2002) Gm*ZIP1* encodes a symbiosis-specific zinc transporter in soybean. J Biol Chem **277:** 4738–4746

**Muchhal US, Pardo JM, Raghothama KG** (1996) Phosphate transporters from the higher plant *Arabidopsis thaliana.* Proc Natl Acad Sci USA **93:** 10519–10523

**Oleski N, Mahdavi P, Bennett AB** (1987) Transport properties of the tomato fruit tonoplast. II. Citrate transport. Plant Physiol **84:** 997–1000

**Pao SS, Paulsen IT, Saier MH** (1998) Major facilitator superfamily. Microbiol Mol Biol Rev **62:** 1–34

**Papoyan A, Kochian LV** (2004) Identification of *Thlaspi caerulescens* genes that may be involved in heavy metal hyperaccumulation and tolerance. Characterization of a novel heavy metal transporting ATPase. Plant Physiol **136:** 3814–3823

**Pence NS, Larsen PB, Ebbs SD, Letham DL, Lasat MM, Garvin DF, Eide D, Kochian LV** (2000) The molecular physiology of heavy metal transport in the Zn/Cd hyperaccumulator *Thlaspi caerulescens.* Proc Natl Acad Sci USA **97:** 4956–4960

**Pittman JK** (2005) Managing the manganese: molecular mechanisms of manganese transport and homeostasis. New Phytol **167:** 733–742

**Poschenrieder C, Tolra R, Barcelo J** (2006) Can metals defend plants against biotic stress? Trends Plant Sci **11:** 288–295

**Ren Q, Paulsen IT** (2005) Comparative analyses of fundamental differences in membrane transport capabilities in prokaryotes and eukaryotes. PLoS Comput Biol **1:** e27

**Rentsch D, Martinoia E** (1991) Citrate transport into barley mesophyll vacuoles—comparison with malate-uptake activity. Planta **184:** 532–537

**Salt DE, Prince RC, Baker AJM, Raskin I, Pickering IJ** (1999) Zinc ligands in the metal hyperaccumulator *Thlaspi caerulescens* as determined using x-ray absorption spectroscopy. Environ Sci Technol **33:** 713–717

**Salt DE, Wagner GJ** (1993) Cadmium transport across tonoplast of vesicles from oat roots. Evidence for a $Cd^{2+}/H^{+}$ antiport activity. J Biol Chem **268:** 12297–12302

**Sarret G, Saumitou-Laprade P, Bert V, Proux O, Hazemann J-L, Traverse A, Marcus MA, Manceau A** (2002) Forms of zinc accumulated in the hyperaccumulator *Arabidopsis halleri.* Plant Physiol **130:** 1815–1826

**Sauer N, Stolz J** (1994) Suc1 and Suc2—two sucrose transporters from *Arabidopsis thaliana* - expression and characterization in bakers yeast and identification of the histidine-tagged protein. Plant J **6:** 67–77

**Shaul O, Hilgemann DW, de-Almeida-Engler J, Van Montagu M, Inzé D, Galili G** (1999) Cloning and characterization of a novel $Mg^{2+}/H^{+}$ exchanger. EMBO J **18:** 3973–3980

**Shimada T, Nakano R, Shulaev V, Sadka A, Blumwald E** (2006) Vacuolar citrate/$H^{+}$ symporter of citrus juice cells. Planta **224:** 472–480

**Simmons CR, Fridlender M, Navarro PA, Yalpani N** (2003) A maize defense-inducible gene is a major facilitator superfamily member related to bacterial multidrug resistance efflux antiporters. Plant Mol Biol **52:** 433–446

**Smith FW, Ealing PM, Dong B, Delhaize E** (1997) The cloning of two Arabidopsis genes belonging to a phosphate transporter family. Plant J **11:** 83–92

**Stolz J, Stadler R, Opekarova M, Sauer N** (1994) Functional reconstitution of the solubilized *Arabidopsis thaliana* Stp1 monosaccharide-$H^{+}$ symporter in lipid vesicles and purification of the histidine-tagged protein from transgenic *Saccharomyces cerevisiae.* Plant J **6:** 225–233

**Talke IN, Hanikenne M, Kramer U** (2006) Zinc-dependent global transcriptional control, transcriptional deregulation, and higher gene copy number for genes in metal homeostasis of the hyperaccumulator *Arabidopsis halleri.* Plant Physiol **142:** 148–167

**Tsay YF, Schroeder JI, Feldmann KA, Crawford NM** (1993) The herbicide sensitivity gene *Chl1* of Arabidopsis encodes a nitrate-inducible nitrate transporter. Cell **72:** 705–713

**Vallee BL, Auld DS** (1990) Zinc coordination, function, and structure of zinc enzymes and other proteins. Biochemistry **29:** 5647–5659

**van der Zaal BJ, Neuteboom LW, Pinas JE, Chardonnens AN, Schat H, Verkleij JA, Hooykaas PJ** (1999) Overexpression of a novel Arabidopsis gene related to putative zinc-transporter genes from animals can lead to enhanced zinc resistance and accumulation. Plant Physiol **119:** 1047–1055

**Verret F, Gravot A, Auroy P, Leonhardt N, David P, Nussaume L, Vavasseur A, Richaud P** (2004) Overexpression of At*HMA4* enhances root-to-shoot translocation of zinc and cadmium and plant metal tolerance. FEBS Lett **576:** 306–312

**Verret F, Gravot A, Auroy P, Preveral S, Forestier C, Vavasseur A, Richaud P** (2005) Heavy metal transport by AtHMA4 involves the N-terminal degenerated metal binding domain and the C-terminal His11 stretch. FEBS Lett **579:** 1515–1522

**Wang J, Evangelou BP, Nielsen MT, Wagner GJ** (1991) Computer-simulated evaluation of possible mechanisms for quenching heavy metal ion activity in plant vacuoles: I. Cadmium. Plant Physiol **97:** 1154–1160

**Wang J, Evangelou BP, Nielsen MT, Wagner GJ** (1992) Computer-simulated evaluation of possible mechanisms for sequestering metal ion activity in plant vacuoles: II. Zinc. Plant Physiol **99:** 621–626

**Wintz H, Fox T, Wu YY, Feng V, Chen WQ, Chang HS, Zhu T, Vulpe C** (2003) Expression profiles of *Arabidopsis thaliana* in mineral deficiencies reveal novel transporters involved in metal homeostasis. J Biol Chem **278:** 47644–47653

**Yamaguchi A, Iwasakiohba Y, Ono N, Kanekoohdera M, Sawai T** (1991) Stoichiometry of metal-tetracycline/$H^{+}$ antiport mediated by transposon Tn10-encoded tetracycline resistance protein in *Escherichia coli.* FEBS Lett **282:** 415–418

**Yamaguchi A, Ono N, Akasaka T, Noumi T, Sawai T** (1990) Metal-tetracycline/$H^{+}$ antiporter of *Escherichia coli* encoded by a transposon, Tn10—the role of the conserved dipeptide, Ser65-Asp66, in tetracycline transport. J Biol Chem **265:** 15525–15530

**Yun CW, Ferea T, Rashford J, Ardon O, Brown PO, Botstein D, Kaplan J, Philpott CC** (2000) Desferrioxamine-mediated iron uptake in *Saccharomyces cerevisiae*—evidence for two pathways of iron uptake. J Biol Chem **275:** 10709–10715

**Yun CW, Tiedeman JS, Moore RE, Philpott CC** (2000) Siderophore-iron uptake in *Saccharomyces cerevisiae*—identification of ferrichrome and fusarinine transporters. J Biol Chem **275:** 16354–16359